THE AMERICAN SOCIETY OF MECHANICAL ENGINEERS
345 E. 47th St., New York, N.Y. 10017

97-AA-10

PERFORMANCE MEASUREMENTS IN LARGE AND SMALL SCALE MULTI-STAGE AXIAL COMPRESSORS

Ulrich Waitke
ABB Power Generation Ltd
Baden, Switzerland

Michael Ladwig
ABB Power Generation Ltd
Baden, Switzerland

SUMMARY

During the commissioning of the prototype of the sequential combustion turbine GT24 extensive measurements of the compressor performance at design- and off-design-operation were accomplished besides the investigation of the other components of the GT. While the compressor performance at design operating conditions was as expected the data obtained showed some unexpected deviations from previously performed measurements of a 1/3-scale test rig of the low pressure compressor. This paper summarizes the results of the measurements and presents a detailed comparison between the measured performance of the GT compressor, the design data and the test rig. The discussion is focused on the influence of scaling effects on the aerodynamic performance and stage matching with particular emphasis on the Reynolds Number influence at different aerodynamic speeds. Furthermore some aspects of the starting behavior of the compressor are presented.

INTRODUCTION

The new family of ABB gasturbines, the GT24 (60 Hz) and GT26 (50 Hz), are characterized by a sequential combustion system with a second combustion chamber between the high pressure turbine and the low pressure turbine (Joos et al., 1996). Figure 1 shows a cross section of the upper half of the GT24 with the air intake from the right, the 22-stage compressor, the EV combustor, 1-stage high pressure turbine, SEV-combustor and 4-stage low pressure turbine. This type of thermodynamic cycle combines high specific power, high efficiency and low emissions but requires a fairly high pressure in order to meet the optimum thermodynamic efficiency. Therefore the development of a new compressor with a pressure ratio of 30:1 was necessary in order to meet the requirements of the cycle. This compressor was designed with variable inlet guide vane, vane 1 and vane 2 to meet the requirements for massflow variation and is equipped with airfoils of controlled diffusion type (Meindl et al., 1995). The first 15 stages were tested in a 1/3-scale test rig in order to validate the performance of the design. The test rig was operated at an inlet pressure of 0.5 bar in order to reduce the power consumption which lead to a reynolds number ratio of 6 between GT and rig compressor.

NOMENCLATURE

A	vibration amplitude
m	intake massflow
n	rotational speed
n_a	aerodynamic speed
R	gas constant
Re	Reynolds number
Δ_{IGV}	setting angle of inlet guide vane
η	polytropic efficiency

Subscripts

$()_a$	aerodynamic
$()_{adm}$	admissible
$()_{ref}$	reference

Superscripts

$()^*$	normalized with design value

Abbreviations

EV	environmental combustor
SEV	sequential EV combustor
IGV	inlet guide vane
GT	gas turbine
OL	operating line

Presented at the ASME ASIA '97 Congress & Exhibition
Singapore - September 30-October 2, 1997

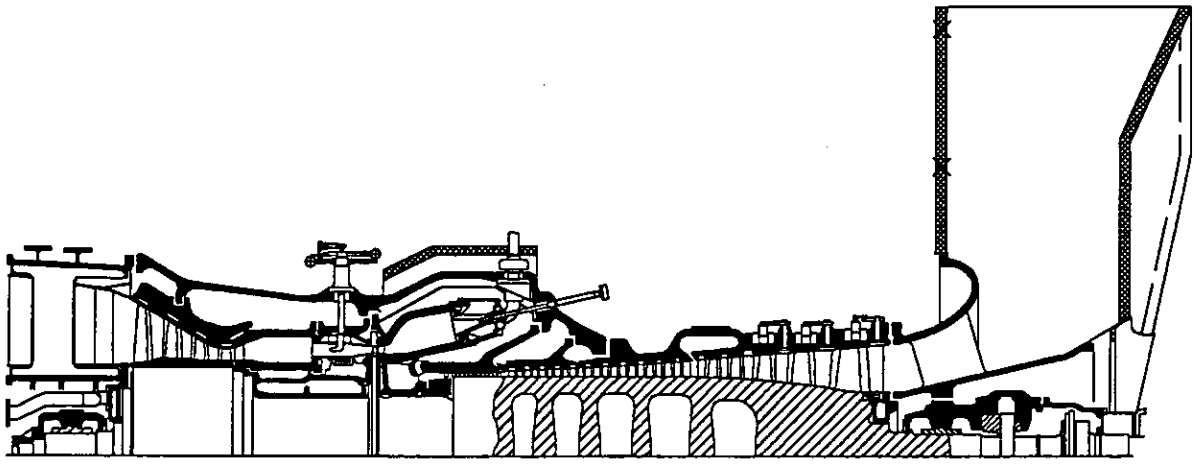

Fig. 1 Cross section of the GT24 gas turbine

PROTOTYPE PERFORMANCE MEASUREMENTS

The intake massflow and efficiency of the "large scale" prototype compressor were investigated in detail during idle and load operating conditions for various aerodynamic speeds and guide vane settings.

The massflow variation as a function of the normalized aerodynamic speed was measured in the prototype engine by means of the static pressure drop along the compressor intake duct. These measurements were carried out during idle operation in a speed range between n_a^*=0.9 and n_a^*=1.08 and under baseload conditions according to the variations of ambient temperature during the commissioning phase. Figure 2 shows the measured mass flow variation of the GT compressor and that of the test rig, scaled to the GT size and inlet conditions. On the first hand the intake massflow of the GT compressor at nominal speed is approximately 1.4% higher than the intake massflow of the rig. This is mainly a Reynolds number effect and was expected to be in this order of magnitude. Furthermore the massflow variation as a function of aerodynamic speed is less in the large scale compressor. This behavior was somewhat unexpected and will be discussed later in more detail.

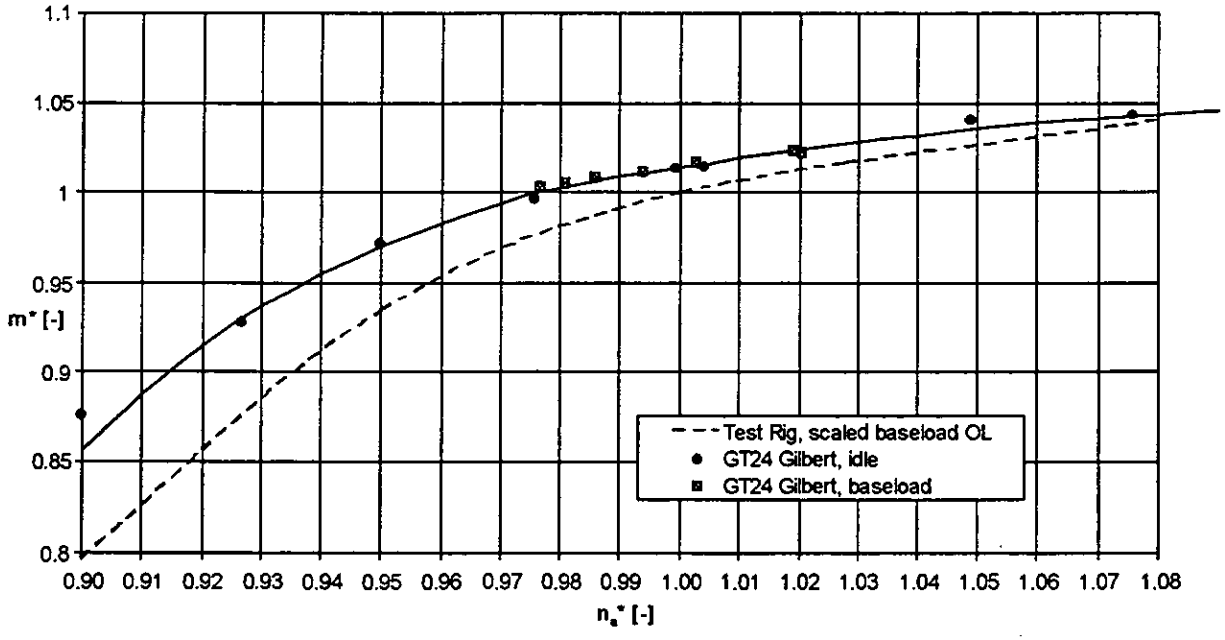

Fig. 2 Massflow variation as a function of normalized aerodynamic speed

The variation of the intake massflow at nominal speed as a function of the setting of the variable guide vanes is shown in fig. 3. The massflow can be reduced to less than 60% of the nominal flow, which provides an optimum means for variation of the GT power output while maintaining the high turbine exhaust temperature and therefore low emissions and high efficiency under off design operation. With the exception of the already mentioned offset at Δ_{IGV}=0°, the behavior of GT and rig compressor are nearly identical.

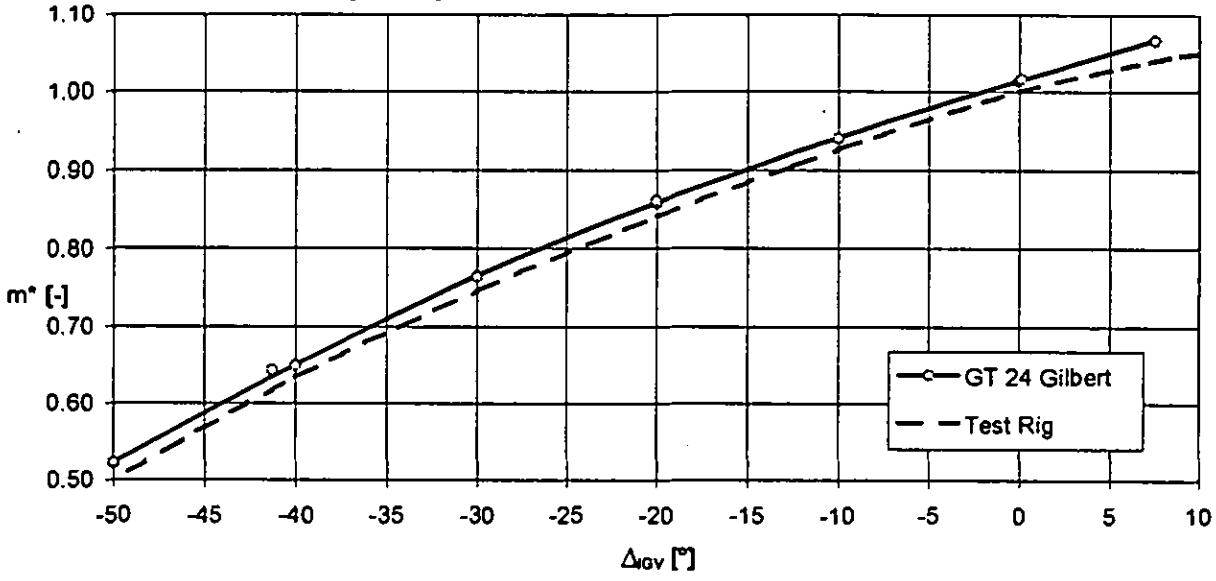

Fig. 3 Massflow variation at nominal speed as a function of IGV setting angle

Figure 4 provides an overview of the measured mass flow variation as a function of variable guide vane settings and aerodynamic speed. As no variation of the mechanical rotational speed was possible during operation under load, most of the measurements were performed during idle operation. As expected, the variation of the intake massflow with aerodynamic speed is reduced for closed guide vanes as the exit Mach number of the inlet guide vane increases and this row becomes dominant for the flow characteristic. For closed guide vanes the influence of the backpressure is neglectable which is also true in the region of high aerodynamic speeds at nominal guide vane setting. The expected reduction of the intake massflow under baseload conditions at low aerodynamic speeds is also shown in the figure.

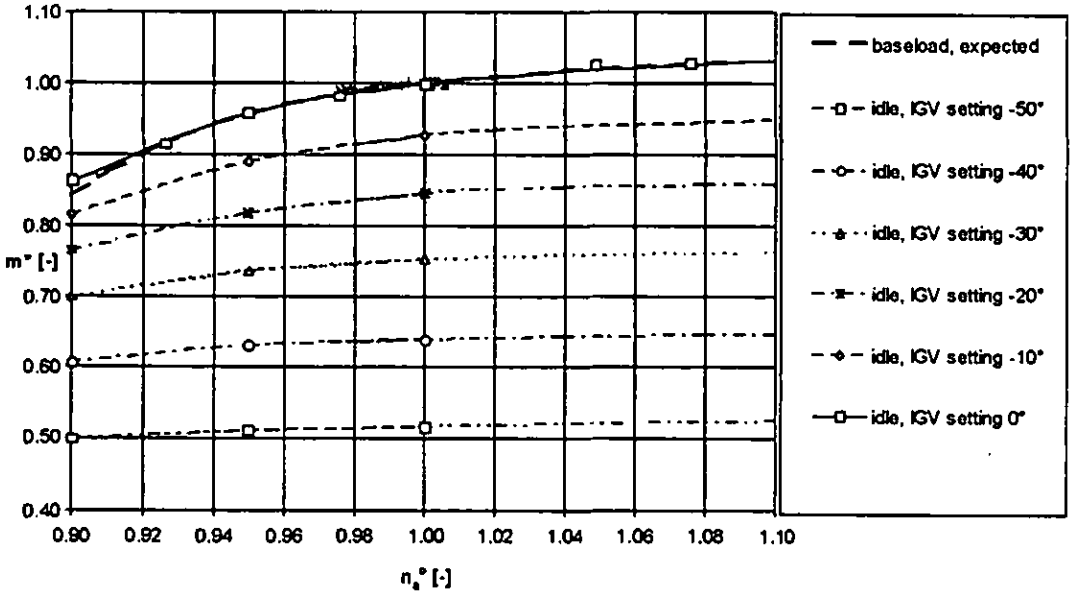

Fig. 4 Massflow variation of the GT compressor as a function of normalized aerodynamic speed and variable guide vane setting

The measured variation of the polytropic efficiency as a function of the aerodynamic speed is shown in fig. 5. The graphs are valid for nominal guide vane setting and a backpressure according to the baseload operating line. Differing from the discussions above the graphs for the GT compressor and the rig are normalized individually, as an accurate measurement of the efficiency in the prototype was available only at the compressor exit, i. e. the graphs refer to the 15-stage rig and the 22-stage GT compressor. Obviously the sensitivity of the GT compressor against changes of aerodynamic speed is significantly higher than expected from the test rig results.

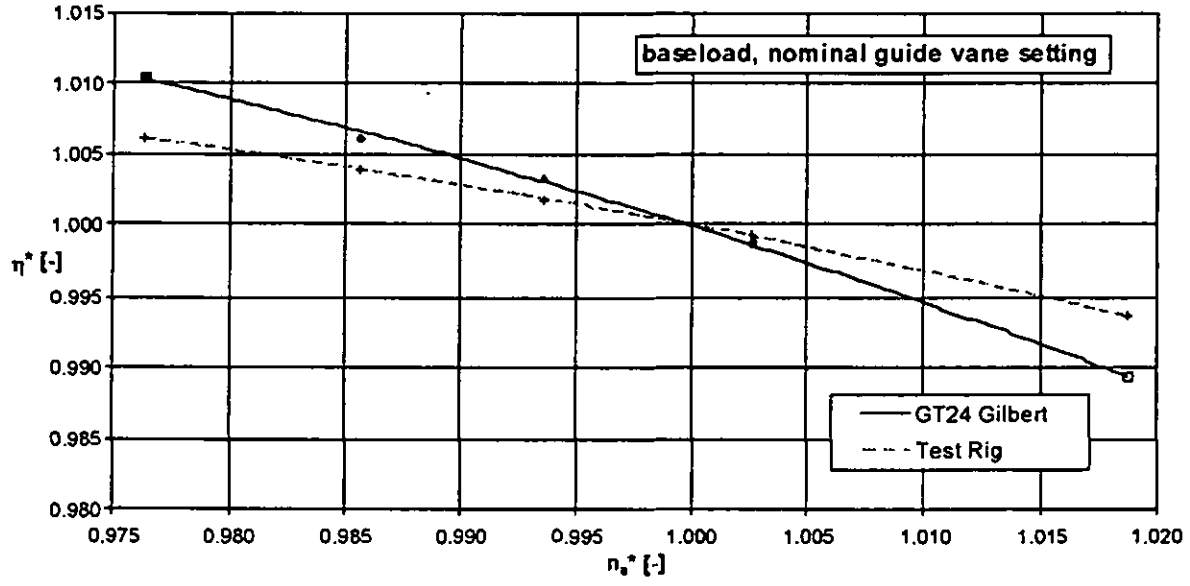

Fig. 5 Efficiency variation as a function of normalized aerodynamic speed

Figure 6 summarizes the results of the efficiency measurements during idle and load operation as a function of the variable guide vane setting angle. While the idle measurements are marked by line graphs, the single dots mark points under loaded conditions according to the operating concept of the gas turbine (Carels et al., 1996). Since for these points an adjustment of the aerodynamic speed was not possible some scatter is visible according to the variation of the ambient conditions during the commissioning. The graphs indicate the good matching of the compressor blading as the optimum efficiency is met at nominal guide vane setting for all aerodynamic speeds except n_a*=0.9. At this condition the higher loading of the front stages causes a drop in efficiency for open guide vanes as the incidence angle of the first rotor approaches the stability limit .

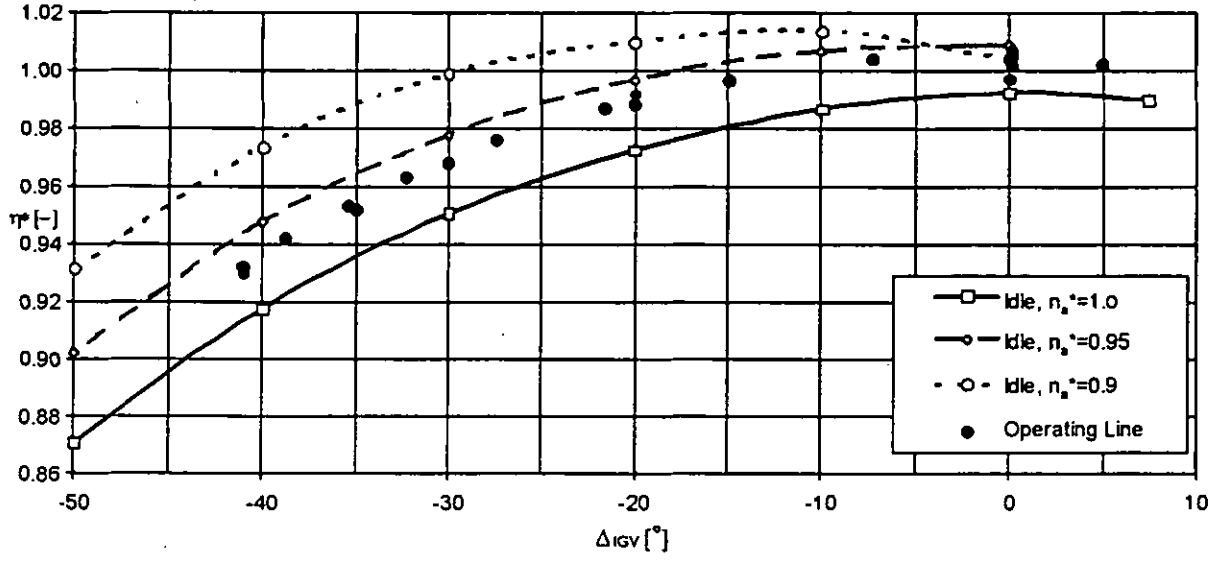

Fig. 6 Efficiency variation of the gas turbine compressor as a function of IGV setting angle

REYNOLDS NUMBER VARIATION IN TEST RIG

The deviations between the test rig and the GT compressor with respect to operation at low aerodynamic speed resulted in a more detailed investigation of the Reynolds number influence in a second rig test in which the intake pressure was varied at nominal guide vane setting for n_a^*= 0.9 and n_a^*=1.0 by throttling the intake duct (Waltke, 1997). A maximum Reynolds number variation by a factor of 2 could be realized by this method. The back pressure was set according to the scaled operating line. The variation of efficiency as a function of the Reynolds number at n_a^*=0.9 is shown in fig. 7. The Reynolds number at the first blade is used as characteristic Reynolds number on the abscissa. The graph is normalized to the efficiency at Re=1.E6. Furthermore the chart contains the graph of a typical correlation (Stoff and Waelchli, 1991).

This correlation is of the form

$$\frac{1-\eta}{1-\eta_{ref}} = \left[\frac{\mathrm{Re}}{\mathrm{Re}_{ref}}\right]^{-n} \qquad (1)$$

Different values for the exponent n can be found in the literature, a value of n=0.125 is most commonly used and is shown in the chart. The agreement of measurement and correlation is quite good in this case.

A different behavior was found for the Reynolds number variation at nominal aerodynamic speed. As shown in fig. 8 the sensitivity of the rig against Reynolds number variations is much less than in the previous case. The sensitivity predicted by the correlation with n=0.125 is too high, a better agreement can be achieved for an exponent of n=0.0555.

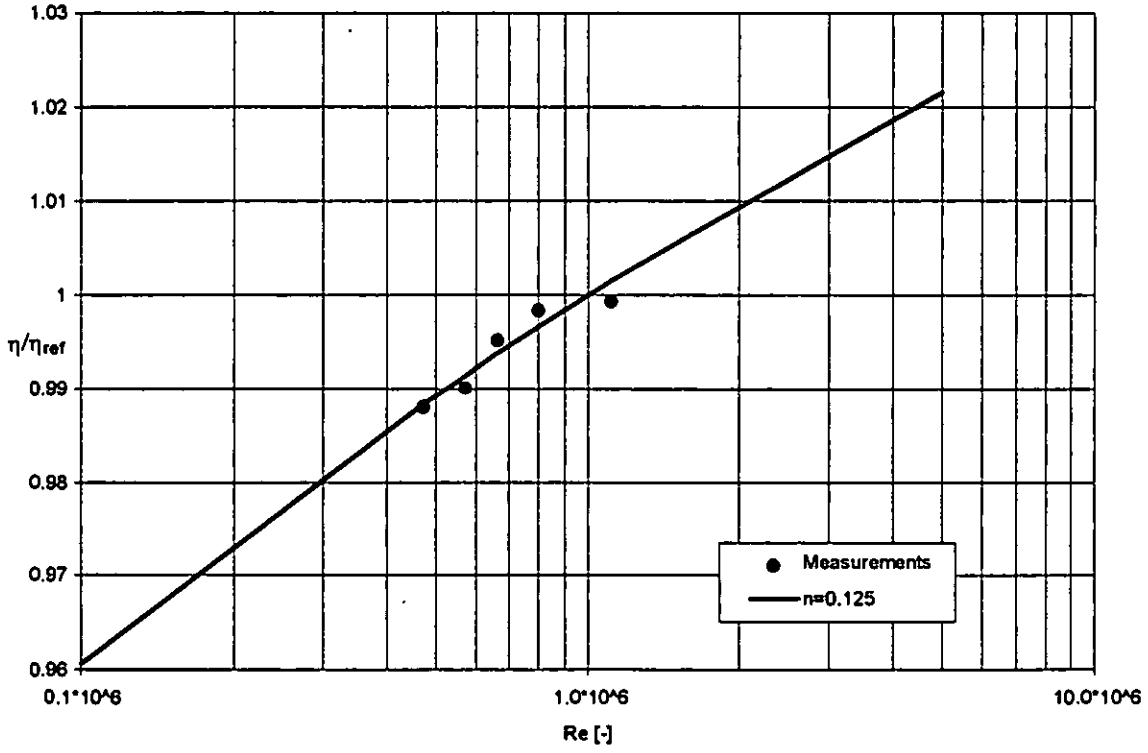

Fig. 7 Efficiency variation of the test rig as a function of Reynolds number at n_a^*=0.9

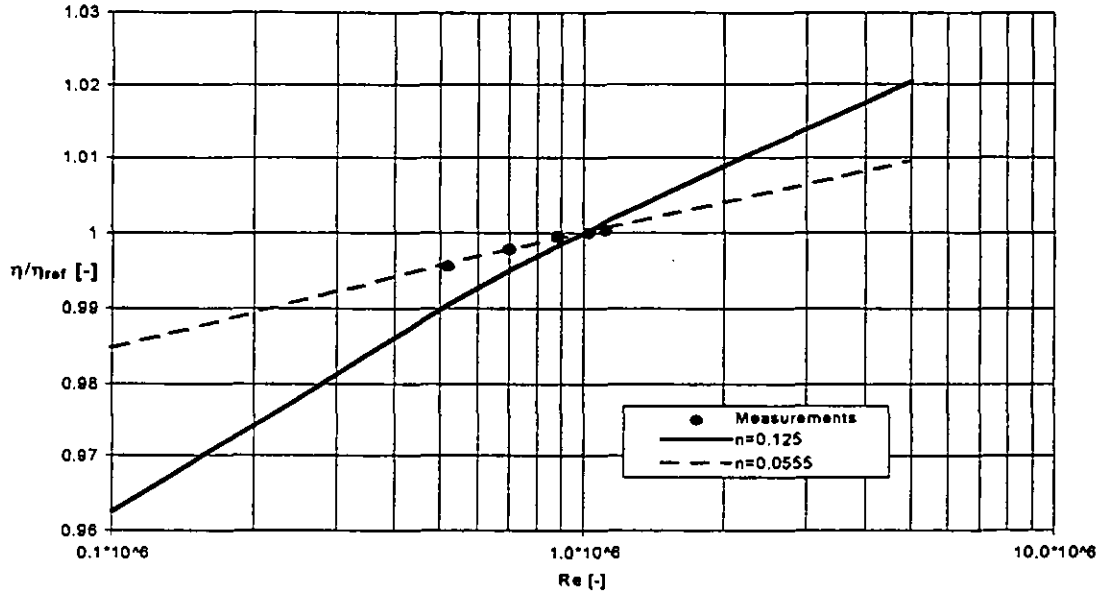

Fig. 8 Efficiency variation of the test rig as a function of Reynolds number at nominal aerodynamic speed

The influence of the Reynolds number on the ingested air flow shows a similar trend. In fig. 9 the variation of the normalized reduced massflow versus Reynolds number is plotted for n_a^*=0.9 and nominal aerodynamic speed. The measured dependency can be correlated by a simple logarithmic function as follows:

$$\frac{m}{m_{ref}} = 1 + a \cdot \ln\left[\frac{\mathrm{Re}}{\mathrm{Re}_{ref}}\right] \qquad (2)$$

The coefficient a was determined as a=0.0415 for n_a^*=0.9. The agreement between measurements and correlation is quite satisfactory. For nominal aerodynamic speed the sensitivity against Reynolds number variation in terms of mass flow is again significantly reduced as was the case for the efficiency. As is shown in fig. 9 the measurements can be correlated quite well by use of a value of 0.0056 for the coefficient a in eq. 2.

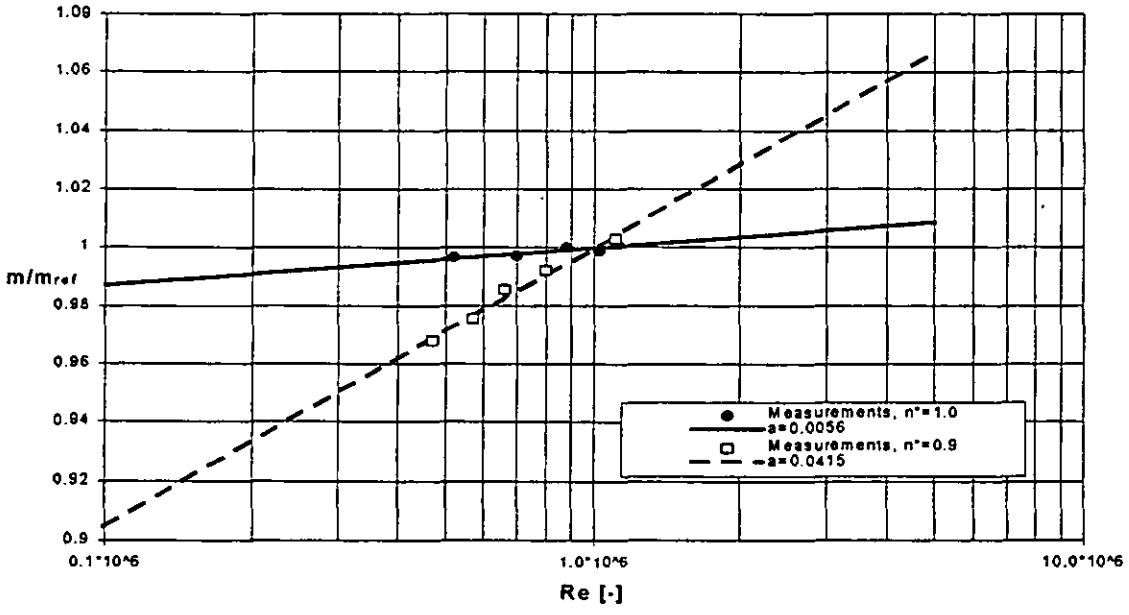

Fig. 9 Massflow variation of the test rig as a function of Reynolds number

A closer investigation of the distribution of the aerodynamic loading of the blading showed that the measured differences in Reynolds number sensitivity are mainly caused by the increased loading of the front stages at low aerodynamic speed.

As is illustrated in fig. 10 the first rotor operates in point A_1 at Reynolds number Re_1 and $n_a^* = 1$ according to the design conditions. Decreasing the Reynolds number to Re_2 shifts the operating point to A_2, resulting in a slight increase of the loss coefficient. Due to the operation near the design conditions the increase of the incidence angle does not affect the loss. The situation changes during operation at low aerodynamic speed. In this case the rotor operates at point B_1 for the high Reynols number. Decreasing Re shifts the operating point towards B_2 in the region of the steep loss increase. In this region the rotor is much more sensitive against changes of the incidence angle and therefore reacts with a higher loss variation.

The deviations of rig and GT results can completelely be explained by this difference in Reynolds number sensitivity. In particular it has to be pointed out that the variation of the Reynolds number during rig tests provides a means to more accurately predict the scaling effects for a given geometric design at different operating conditions.

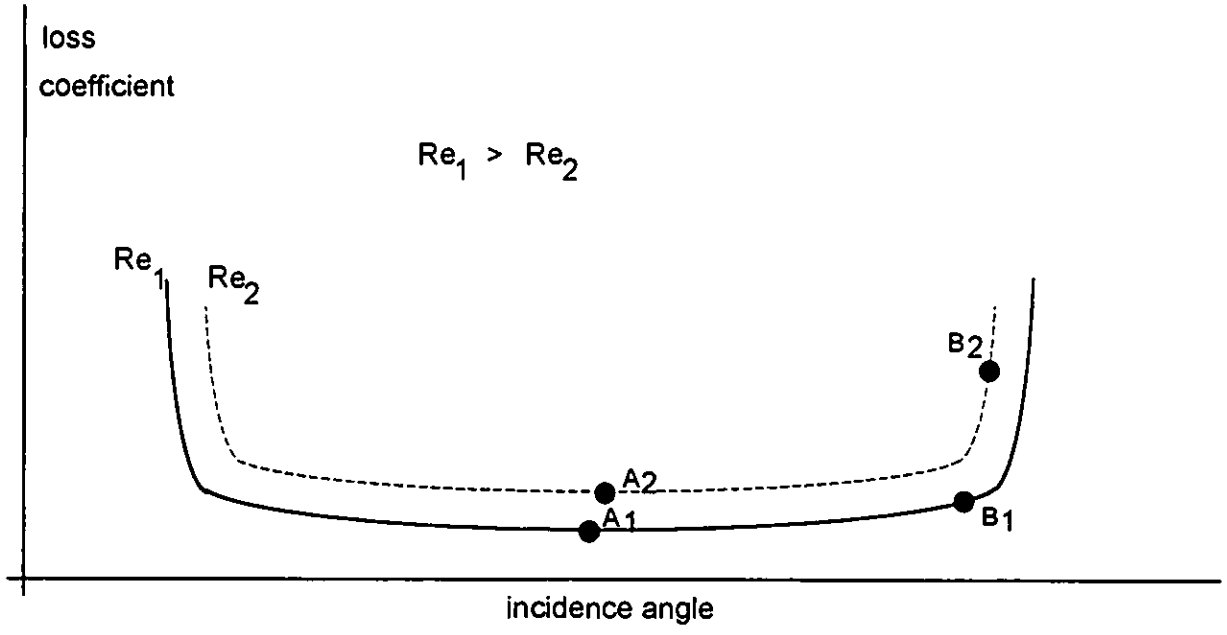

Fig. 10 Profile loss as function of incidence angle for different Reynolds numbers

STARTUP MEASUREMENTS

During the early commissioning phase the GT24 compressor in Gilbert suffered from a rotating stall which caused an excitation of the shaft during startup. By adding an additional blow off device at stage 11 the stall could be drastically reduced, subsequently enabling a smooth and fast runup. As an example the shaft vibrations at the compressor bearing are shown in fig. 11 for a typical start.

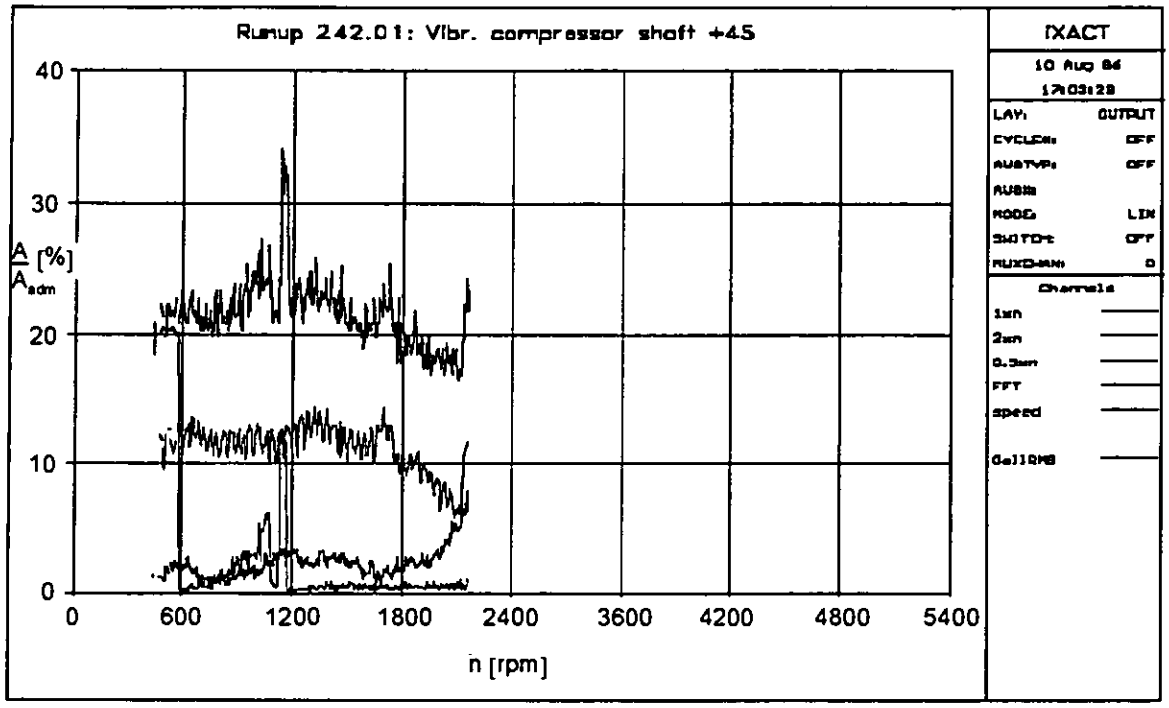

Fig. 11 Shaft vibrations at compressor bearing for typical start

SUMMARY

The compressor of the first GT24 at Gilbert Generating Station, NJ, USA, was investigated in detail during the commissioning phase. A comparison with earlier accomplished rig tests showed some unexpected differences in the off-design characteristics of the rig and the GT compressor. The reason for these deviations could be identified by a second series of rig tests as a strong dependency of the Reynolds number sensitivity on aerodynamic speed. During the first run-ups the GT compressor suffered from rotating stall which could be reduced by optimization of the blow-off system. The results of the commissiong measurements prove the wide operation range as well as the safe operation of the compressor under all operating conditions required by the advanced cycle concept.

ACKNOWLEDGMENTS

The Reynolds number investigations were performed as part of a project partially funded by the German Ministry of Education, Science, Research and Technology (contract no. 0326820D) in the frame of the AG TURBO research program. On behalf of ABB Power Generation this support is gratefully acknowledged.

REFERENCES

Carels, Y., Ladwig, M., Marchmont, C., Meier, R., 1996, "Commissioning, Testing and Validation of ABB's GT24 at JCP&L's Gilbert Generating Station", paper presented at Power Gen Asia, New Delhi, sept. 1996

Joos, F. , Brunner, P., Schulte-Werning, B., Syed, K. and Eroglu, A., 1996, "Development of the Sequential Combustion System for the ABB GT24/GT26 Gas Turbine Family", ASME-paper 96-GT-315.

Meindl, T., Farkas, F., Klussmann, W, 1995, "The Development of a Multi-Stage Compressor for Heavy Duty Industrial Gas Turbines", ASME-paper 95-GT-371.

Stoff, H. and Waelchli, R., 1991, "Aufwertung des Wirkungsgrades von Gasturbinen-Axialverdichterbeschaufelungen ueber den Einfluss der Reynoldszahl", Forschung im Ingenieurwesen 57, No. 5.

Waltke, U., 1997, "Untersuchung der Endstufen eines vielstufigen Axialverdichters mit CDA-Beschaufelung", AG Turbo project no. 0326 820 D, final report.